

# Internship report

Enzo Isnard

August 31, 2021

## Contents

<b>1</b>	<b>Introduction</b>	<b>2</b>
<b>2</b>	<b>Maxwell's equations</b>	<b>2</b>
<b>3</b>	<b>FDTD in 1D</b>	<b>3</b>
3.1	Presentation of the scheme: . . . . .	3
3.2	Stability Condition . . . . .	3
3.3	Normalized equations . . . . .	4
3.4	Absorbing boundary conditions . . . . .	5
3.4.1	Mur's ABC . . . . .	5
3.5	Tests on a dielectric slab . . . . .	6
3.6	Instantaneous frequency . . . . .	9
3.6.1	Definition and methods to compute it . . . . .	9
3.6.2	Analytical solutions and comparisons with the numerical ones . . . . .	10
3.7	Comparison with analytical solutions of E . . . . .	14
3.7.1	Analytical solutions in free space . . . . .	14
3.7.2	Analytical solutions in time-varying media . . . . .	17
<b>4</b>	<b>Discontinuous Galerkin method in 1D</b>	<b>20</b>
4.1	Re-normalized equations . . . . .	20
4.2	Conservative form . . . . .	20
4.3	Weak formulation . . . . .	21
4.4	Space discretization . . . . .	21
4.5	Matrix formulation . . . . .	22
4.6	Comparison with FDTD . . . . .	24
4.7	Test on a dielectric case . . . . .	26
<b>5</b>	<b>Conclusion</b>	<b>28</b>

# 1 Introduction

The goal is to simulate Maxwell's equations using the FDTD scheme and compare the results with Discontinuous Galerkin method.

## 2 Maxwell's equations

The Maxwell's equations in continuous media are the following:

$$\begin{aligned}\nabla \cdot \mathbf{D} &= \rho \\ \nabla \cdot \mathbf{B} &= 0 \\ \nabla \times \mathbf{E} &= -\partial_t \mathbf{B} \\ \nabla \times \mathbf{H} &= \mathbf{J} + \partial_t \mathbf{D}\end{aligned}$$

We can derive from these equation the continuity equation, that states that the charges move continuously.

$$\nabla \cdot \mathbf{J} + \partial_t \rho = 0$$

We also have 3 relations between the different fields

$$\begin{aligned}\mathbf{D} &= \epsilon \mathbf{E} \\ \mathbf{B} &= \mu \mathbf{H} \\ \mathbf{J}_c &= \sigma \mathbf{E}\end{aligned}$$

$\mathbf{J}_c$  is the current density created by the electromagnetic fields. We will note  $\mathbf{J}_s = \mathbf{J} - \mathbf{J}_c$  the current density created by external sources. In general  $\epsilon$ ,  $\mu$  and  $\sigma$  are second rank tensors, but here we will consider that they are scalars. We will consider that  $\epsilon$  can vary in time and space,  $\mu$  equal to  $\mu_0$  and  $\sigma$  equal to 0. Maxwell's equations become:

$$\begin{aligned}\nabla \cdot (\epsilon \mathbf{E}) &= \rho \\ \nabla \cdot \mathbf{H} &= 0 \\ \nabla \times \mathbf{E} &= -\mu_0 \partial_t \mathbf{H} \\ \nabla \times \mathbf{H} &= \partial_t \mathbf{D} + \mathbf{J}_s\end{aligned}$$

The first two equations are called the auxiliary equations because they don't change in time, we can in fact show taking the divergence of the curl equations and using the continuity equation that:

$$\begin{aligned}\partial_t (\nabla \cdot \mathbf{B}) &= 0 \\ \partial_t (\nabla \cdot \mathbf{D} - \rho) &= 0\end{aligned}$$

Hence if they are verified initially, they will be verified in the futures states, so we don't need to include them in the FDTD scheme.

### 3 FDTD in 1D

#### 3.1 Presentation of the scheme:

In this part we will consider the Maxwell's equations in one dimension and introduce the FDTD scheme in this case. We suppose that  $\mathbf{E}$  has only a component along  $z$  and that  $\mathbf{H}$  has only a component along  $y$ . We also suppose that these two components only depend on  $x$ . In this case Maxwell's equations become:

$$\begin{cases} \partial_x E_z(t, x) &= \mu_0 \partial_t H_y(t, x) \\ \partial_x H_y(t, x) &= \partial_t (\epsilon(t, x) E_z(t, x)) + J_s \end{cases}$$

The idea of FDTD is to use central finite difference to discretize the derivatives and to alternately compute  $E_z$  and  $H_y$ , as presented in the figure below:

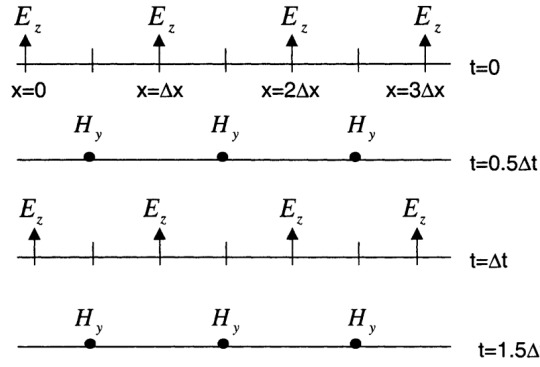


Fig 3.2 in [2]

This leads us to the scheme presented in [2] at p.32:

$$\begin{aligned} E_z^{n+1}(i) &= \frac{\epsilon^{n+1}(i)}{\epsilon^n(i)} E_z^n(i) + \frac{\Delta t}{\epsilon^{n+1}(i) \Delta x} (H_y^{n+1/2}(i+1/2) - H_y^{n+1/2}(i-1/2)) + E_s^{n+1}(i) \\ H_y^{n+3/2}(i+1/2) &= H_y^{n+1/2}(i+1/2) + \frac{\Delta t}{\mu_0 \Delta x} (E_z^{n+1}(i+1) - E_z^{n+1}(i)) \end{aligned}$$

where  $i$  is the spatial index,  $n$  the time index and  $E_s^n(i)$  is the source electric field (it is related to the source current density by  $E_s^n(i) = -\frac{\Delta t}{\epsilon^{n+1}(i)} J_s^{n+1}(i)$ ).

#### 3.2 Stability Condition

It can be shown that in order to be stable, the time step and the space step need to verify the Courant's condition, which is:

$$\frac{c_0 \Delta t}{\Delta x} \leq 1$$

where  $c_0 = \frac{1}{\sqrt{\epsilon_0 \mu_0}}$  is the speed of light in free space. This ratio is often called the Courant's number or the cfl number and we will note it  $C_s$ .

### 3.3 Normalized equations

In order to simplify the update equations and to have  $H_y$  and  $E_z$  with the same order of magnitude we use a normalized version of  $\mathbf{E}$ :  $\tilde{E}_z = Y_0 E_z = \sqrt{\frac{\epsilon_0}{\mu_0}} E_z$ .

We also use the relative electric permittivity:  $\epsilon_r^n(i) = \frac{\epsilon^n(i)}{\epsilon_0}$ .

We obtain the following simplified equations:

$$\begin{aligned} \tilde{E}_z^{n+1}(i) &= \frac{\epsilon_r^n(i)}{\epsilon_r^{n+1}(i)} \tilde{E}_z^n(i) + \frac{C_s}{\epsilon_r^{n+1}(i)} [H_y^{n+1/2}(i+1/2) - H_y^{n+1/2}(i-1/2)] + \tilde{E}_s^{n+1}(i) \\ H_y^{n+3/2}(i+1/2) &= H_y^{n+1/2}(i) + C_s [\tilde{E}_z^{n+1}(i) - \tilde{E}_z^{n+1}(i+1)] \end{aligned}$$

### 3.4 Absorbing boundary conditions

#### 3.4.1 Mur's ABC

We use absorbing boundary conditions (ABC) to make as if our domain was infinite. The Mur's ABCs are the most commonly used in FDTD, they are:

$$E_z^{n+1}(0) = E_z^n(1) + \frac{v_{fs}\Delta t - \Delta x}{v_{fs}\Delta t + \Delta x} [E_z^{n+1}(1) - E_z^n(0)]$$
$$E_z^{n+1}(i_{max}) = E_z^n(i_{max} - 1) + \frac{v_{fs}\Delta t - \Delta x}{v_{fs}\Delta t + \Delta x} [E_z^{n+1}(i_{max} - 1) - E_z^n(i_{max})]$$

where  $v_{fs}$  is the speed of the wave at the boundary, in our case  $v_{fs} = c_0$ , and using the fact that  $c_0\Delta t = C_s\Delta x$  we get:

$$\tilde{E}_z^{n+1}(0) = \tilde{E}_z^n(1) + \frac{C_s - 1}{C_s + 1} [\tilde{E}_z^{n+1}(1) - \tilde{E}_z^n(0)]$$
$$\tilde{E}_z^{n+1}(i_{max}) = \tilde{E}_z^n(i_{max} - 1) + \frac{C_s - 1}{C_s + 1} [\tilde{E}_z^{n+1}(i_{max} - 1) - \tilde{E}_z^n(i_{max})]$$

### 3.5 Tests on a dielectric slab

To test if the code we implemented is working the cases presented in [2] in Chapter 3 (p 38).

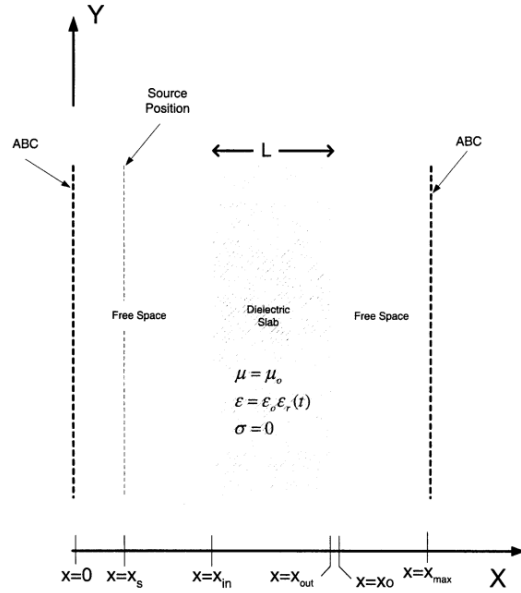


Fig 3.3 in [2]

We use a sinusoidal point source of frequency  $f_s = 10$  GHz. The slab permittivity has sinusoidal variations with time of the form:

$$\epsilon_r(t) = \epsilon_{r0} [1 + b \sin(2\pi f_m t)], \text{ with } f_m = 1 \text{ GHz, } b = 0.67 \text{ and } \epsilon_{r0} = 3.$$

I've tested for both a thin slab ( $L = 3mm$ ) and a thick slab ( $L = 93mm$ ) and here are the results:

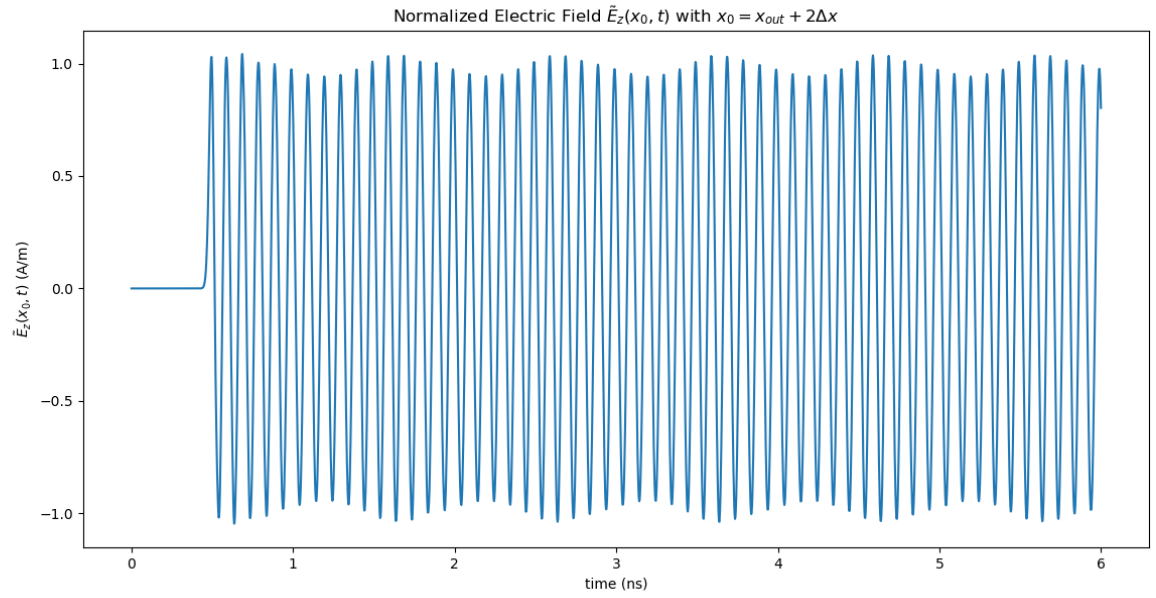


Figure from my program with  $L=3\text{mm}$

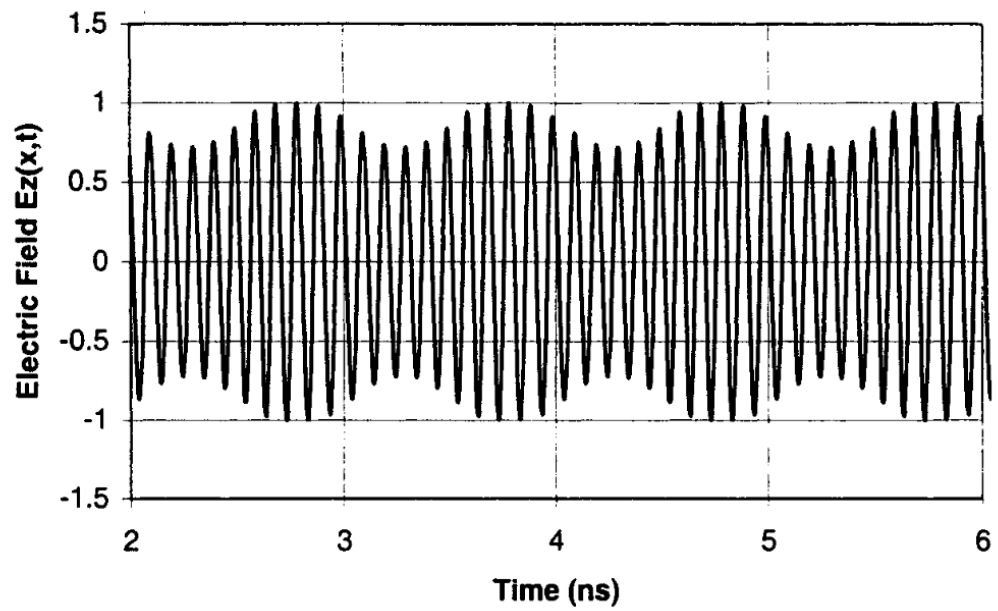


Figure from [2] with  $L=3\text{mm}$ (p 38)

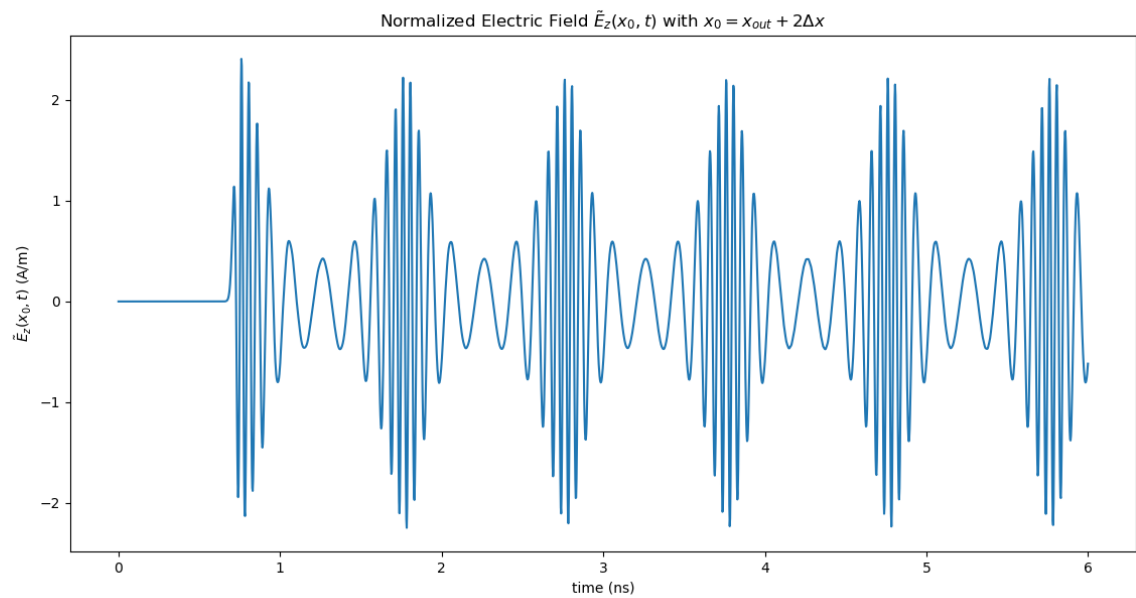


Figure from my program with  $L=93\text{mm}$

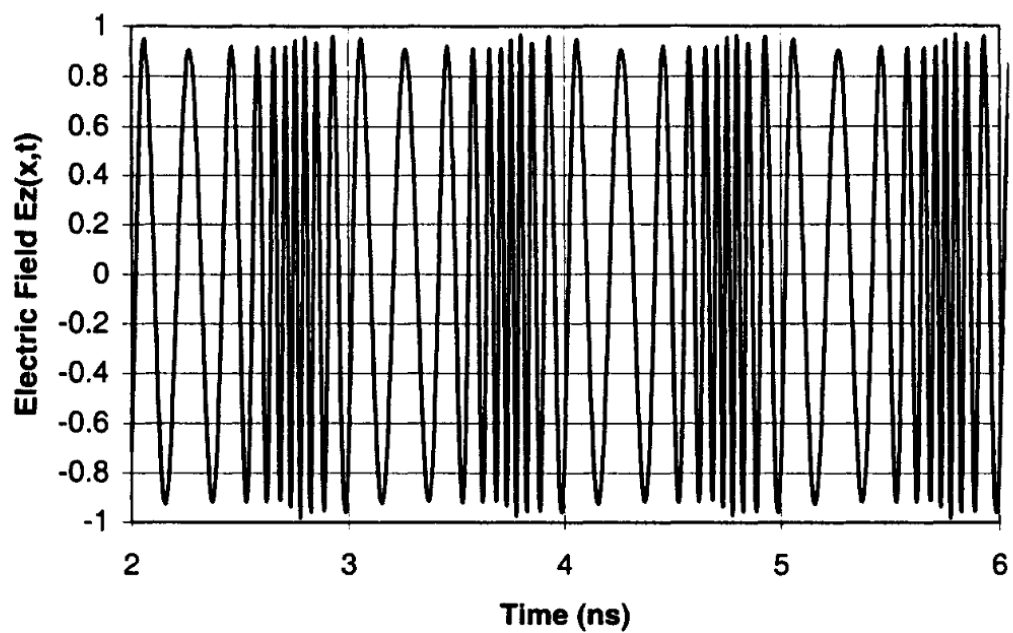
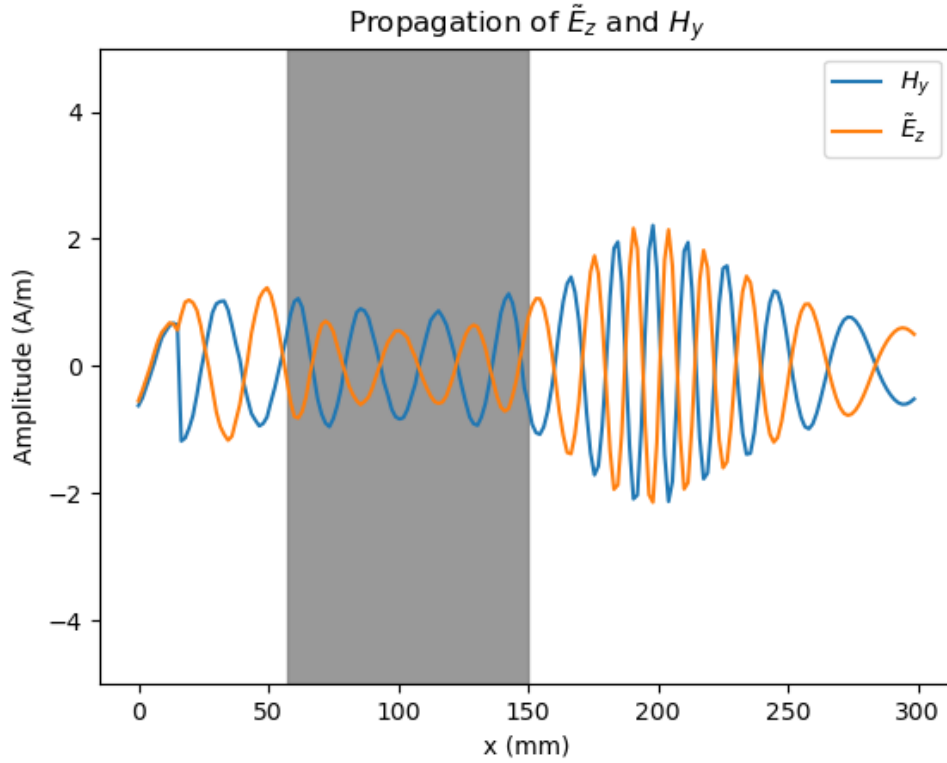


Figure from [2] with  $L=93\text{mm}$  (p 39)



I have similar results for the thin slab but for the thick slab I have a change in amplitude which is not observed in [2]. However the frequencies of the two signals seem similar.

If we plot  $\tilde{E}_z$  as a function of  $x$  instead of  $t$  we can see that the thick slab creates sorts of wave packets in output:



### 3.6 Instantaneous frequency

#### 3.6.1 Definition and methods to compute it

In his phd's thesis Xiaowen Liu doesn't give a close form of the electric field but only of a quantity called the instantaneous frequency that we are going to define.

Intuitively if we have a signal of the form:  $s(t) = A \sin(\phi(t))$  we define the instantaneous phase as being  $\phi(t)$ . The instantaneous frequency is then only by:  $f(t) := \frac{1}{2\pi} \frac{d\phi}{dt}(t)$ .

For a more general signal we need to extend the function to the complex domain, or more precisely to upper-half complex domain. A way to do so is by computing the Hilbert transform of the signal, which is defined by:

$$\mathcal{H}[s](t) := \bar{s}(t) := \frac{1}{\pi t} * s(t) = \frac{1}{\pi} \text{p.v} \int_{-\infty}^{\infty} \frac{s(\tau)}{t - \tau} d\tau$$

where p.v is the Cauchy principal value.  
Then we define the analytical signal of  $s$  by:

$$s_a(t) := s(t) + i\bar{s}(t)$$

The instantaneous phase is then simply the argument of the instantaneous signal:  $\phi(t) := \arg[s_a(t)]$

We can also remark that  $\mathcal{F}[s_a](\omega) = 2H(\omega)\mathcal{F}[s](\omega)$  where  $\mathcal{F}$  is the Fourier transform and  $H$  the Heaviside function. It gives us an easy way to compute the analytical signal numerically by using the *FFT* and the *IFFT* (it is actually the way used in *scipy* to compute the analytical signal).

Xiaowen Liu also presents an alternative way to compute the instantaneous frequency. The method consist in computing the Electric Field at  $x_o$  with the source  $f_s^{(1)}(t) = \sin(\omega_0 t)$  and then recomputing it with the source  $f_s^{(2)}(t) = \cos(\omega_0 t)$ . We denote the sequence of values of the electric field for the 1st source by  $g^{(1)}(n)$  and the one for the 2nd source by  $g^{(2)}(n)$ . The sequence of phase values of the signal is then given by:

$$\phi(n) = \text{atan2}[g^{(1)}(n), g^{(2)}(n)]$$

where  $\text{atan2}$  is the four-quadrant inverse tangent function.

In order to compute the derivative of  $\phi$  a five-point numerical derivative is used, which is:

$$f(n) = \frac{1}{2\pi} \frac{\phi(n-2) - 8\phi(n-1) + 2\phi(n+1) - \phi(n+2)}{2\Delta t}$$

The magnitude of the error of this formula is  $\mathcal{O}(\Delta t^4)$ .

### 3.6.2 Analytical solutions and comparisons with the numerical ones

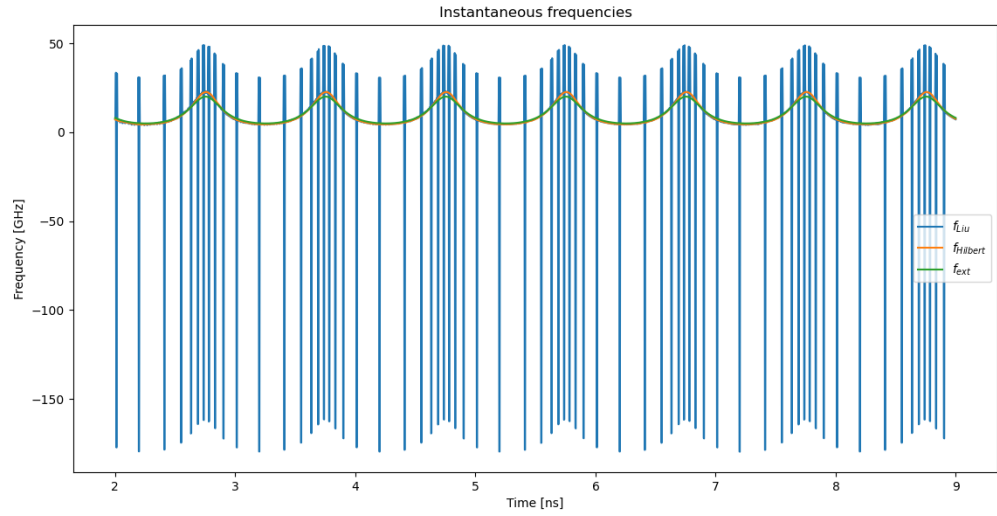
The analytical solution of the instantaneous frequency when the modulation depth  $b$  is way smaller than 2 can be approximated by [2]:

$$f(t) \approx \frac{1}{2\pi} \frac{\sec^2(\omega_m t/2)}{1 + \left[ \frac{2 \tan(\omega_m t/2) + b}{\sqrt{4-b^2}} \right]^2} \frac{\sec^2 \left[ \tan^{-1} \left\{ \frac{2 \tan(\omega_m t/2) + b}{\sqrt{4-b^2}} \right\} - \frac{\omega_m L \sqrt{4-b^2}}{4v_0} \right] \omega_s}{\left[ 1 + \left\{ \frac{\sqrt{4-b^2}}{2} \tan \left[ \tan^{-1} \left\{ \frac{2 \tan(\omega_m t/2) + b}{\sqrt{4-b^2}} \right\} - \frac{\omega_m L \sqrt{4-b^2}}{4v_0} \right] - \frac{b}{2} \right\}^2 \right]}$$

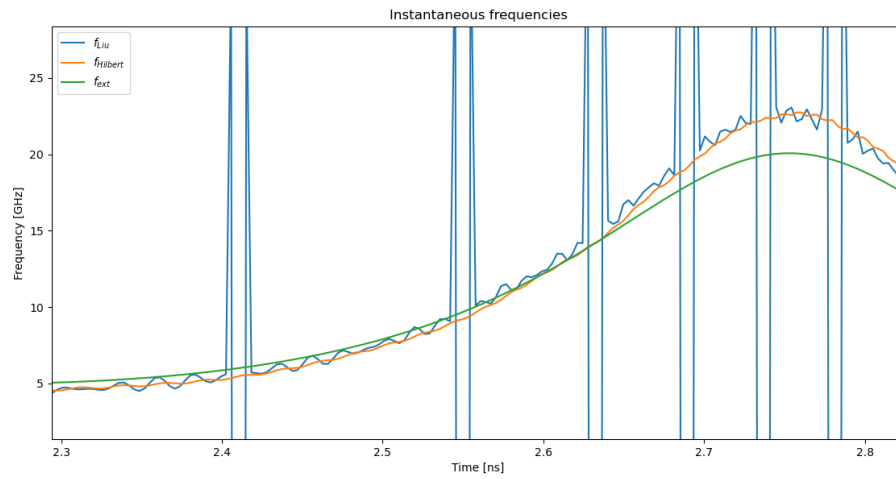
where  $v_0 = \frac{1}{\sqrt{\epsilon_0 \mu_0 \epsilon_{r0}}}$

We can note that if  $L = \frac{4K\pi v_0}{\omega_m \sqrt{4-b^2}} = KL_0$  with  $K \in \mathbb{N}$  then  $f$  is constant and equal to  $\frac{\omega_m}{2\pi}$ .

If we plot the frequencies calculated with Liu's method, FFT and the analytical solution for the thick slab we get:

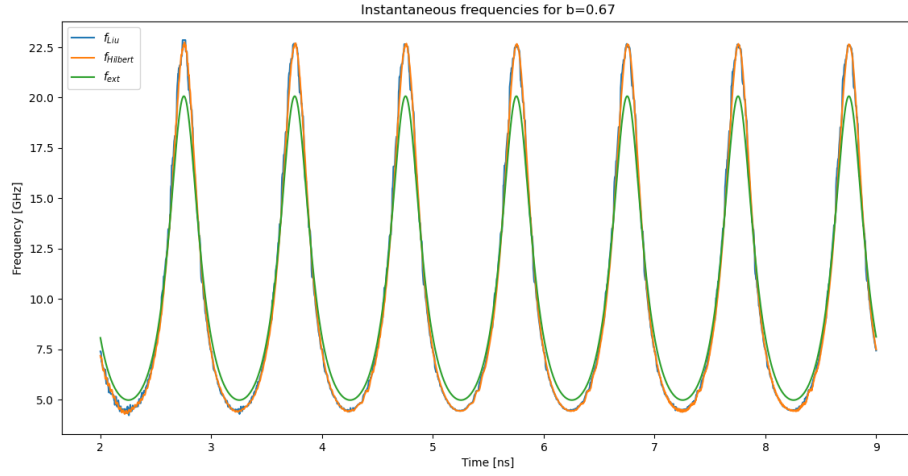


The frequency calculated with Liu's method is very instable. If we zoom in we can see that there is only a few points that have absurd values.

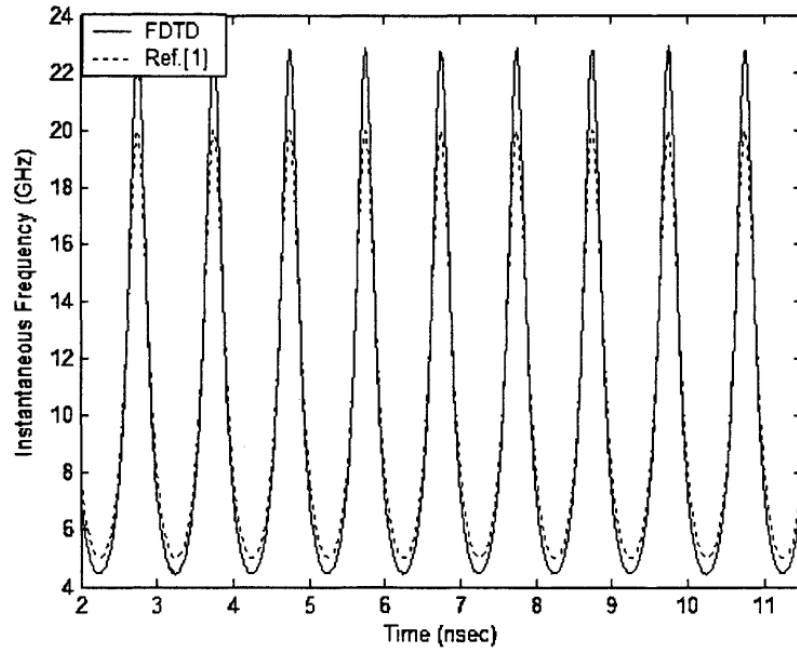


We can remove these absurd values by applying a median filter to this frequency. In the following plots we will take a window of 10 values for the median filter.

After applying this filter we have:

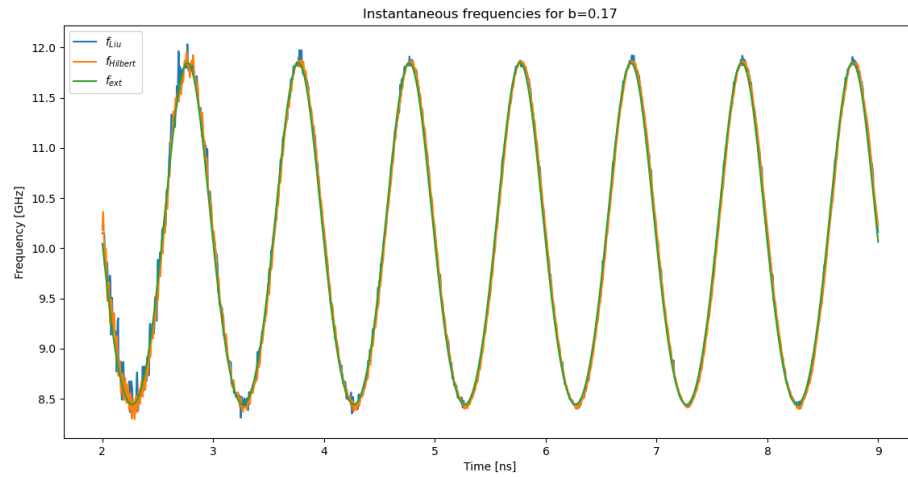


Which is quite similar to the result of [2](p.49):

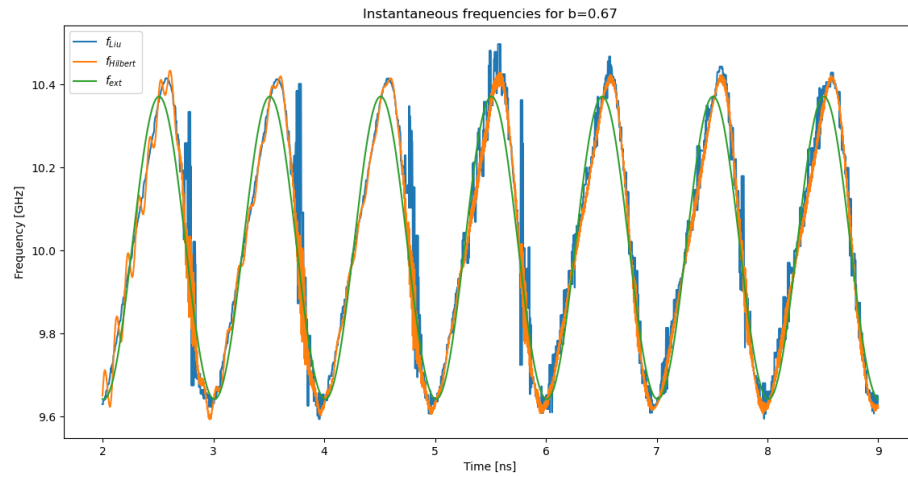


Instantaneous frequencies of the Electric Field at  $x = L + 2\Delta x$  with  $b = 0.67$

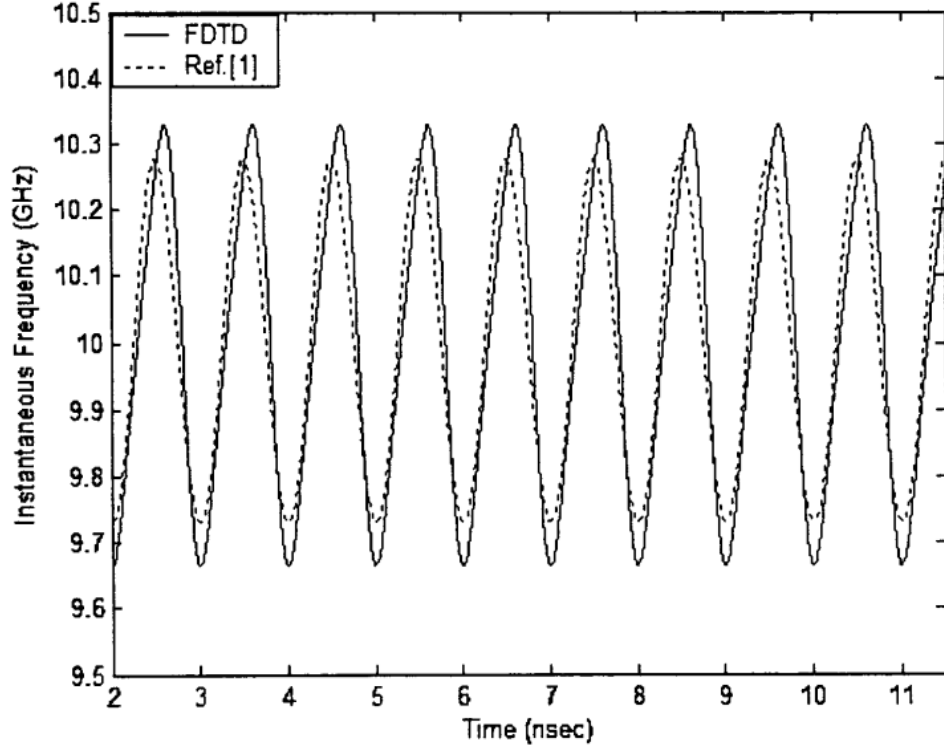
If we reduce the value of  $b$  to 0.17 the frequencies computed with the FDTD algorithm are closer to the analytical one:



For the thin slab we have the following results:



Results with my program



Results in the phd thesis

### 3.7 Comparison with analytical solutions of E

#### 3.7.1 Analytical solutions in free space

In order to measure if our solutions converge effectively I simulated one of the simplest case we can think in 1D, which is the vacuum-filled cavity with metallic boundaries. We take as domain  $\Omega = [0, 1]$  and as initial conditions  $E_z(0, x) = \sin x$  and  $H_y(0, x) = 0$  and for simplicity we will take  $\epsilon_0 = \mu_0 = 1$ . We use Perfect electric conditions (PEC), which in 1D is homogeneous Dirichlet conditions for  $E_z$ . We can proof easily using the separation of variables that the analytical solutions of  $E_z$  and  $H_y$  are:

$$\begin{cases} E_z(t, x) = \sin(\pi x) \cos(\pi t) \\ H_z(t, x) = \cos(\pi x) \sin(\pi t) \end{cases}$$

This case has the particularity to conserve the electromagnetic energy, which is by definition:

$$\mathcal{E}(t) := \frac{1}{2} \int_{\Omega} \mathbf{D} \cdot \mathbf{E} + \mathbf{H} \cdot \mathbf{B} \, dx$$

Its exact value in our case is:

$$\mathcal{E}(t) = \frac{\cos(\pi t)^2}{2} \int_0^1 \sin(\pi x)^2 \, dx + \frac{\sin(\pi t)^2}{2} \int_0^1 \cos(\pi x)^2 \, dx = 1/4$$

In order to compare our numerical solutions to the analytical ones we use the  $L^2$  norm:

$$\|u\|_2^n = \left( \sum_{i=1}^n u^n(i)^2 \Delta x \right)^{1/2}$$

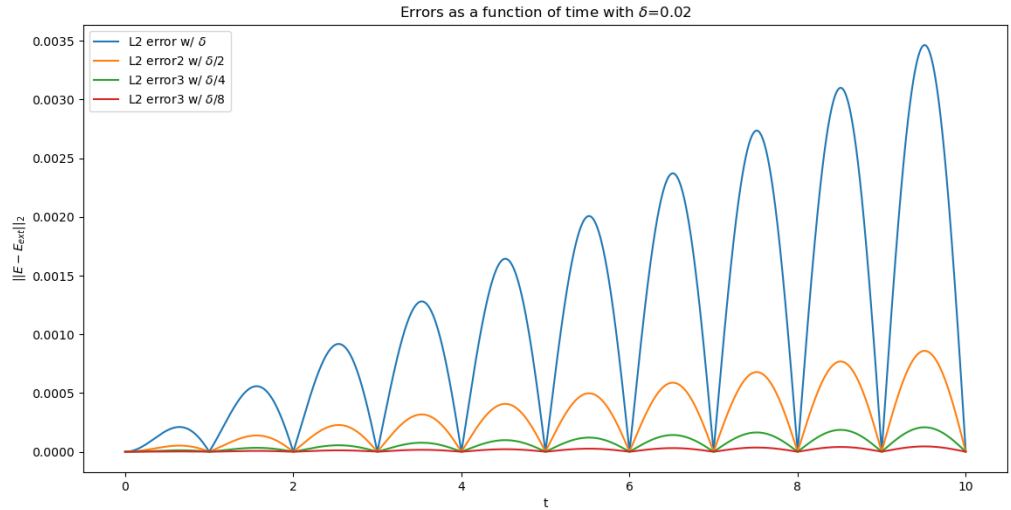
and we will use as error :

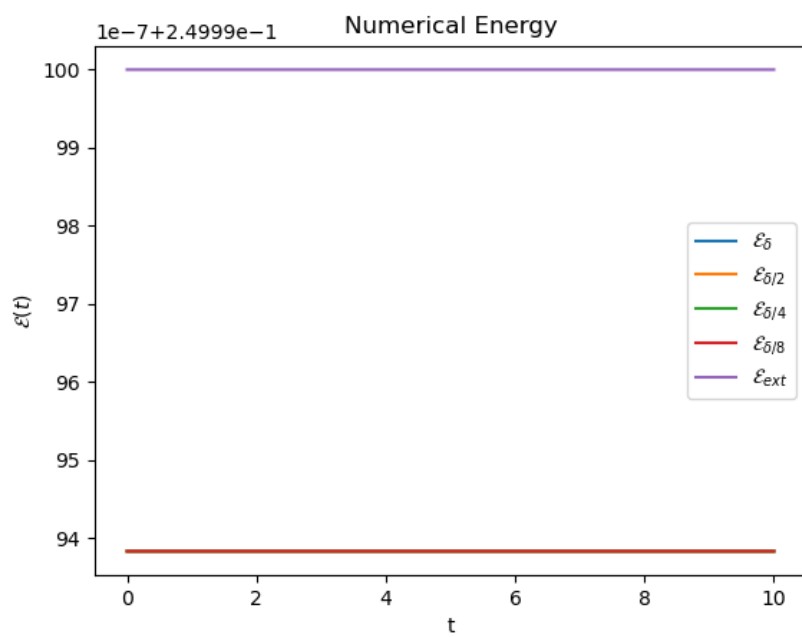
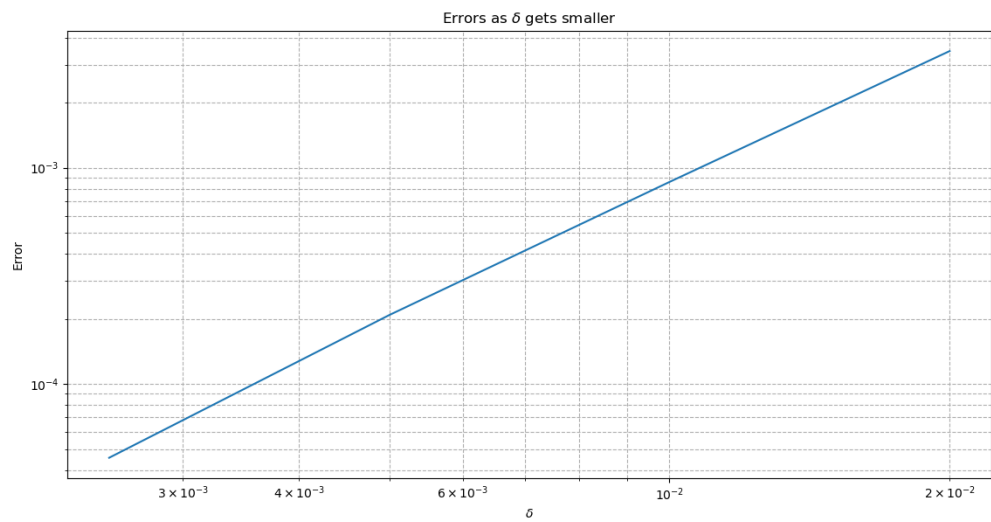
$$\max_n \|u - u_{ext}\|_2^n$$

To compute the energy numerically we use the following formula:

$$\mathcal{E}_{num}(n) = \sum_{i=0}^{i_{max}} \epsilon_r(n) E_z^n(i)^2 + \sum_{i=0}^{i_{max}-1} H_y^{n+\frac{1}{2}}(i + \frac{1}{2}) H_y^{n-\frac{1}{2}}(i + \frac{1}{2})$$

Results with  $\delta = 1/50$  and  $\Delta t = 0.001$





As expected the order of convergence using L2 norm is equal to 2 and the energy is constant.



### 3.7.2 Analytical solutions in time-varying media

As said before [2] only gives analytical solutions for the instantaneous frequency of  $E$  after the dielectric. Nonetheless in a paper about another method based on Magnus Expansion [1] the authors give analytical solutions for  $\mathbf{E}$  when all the domain has a time varying permittivity and with PEC. It allows us to compare directly our result to the analytical solution of  $\mathbf{E}$ .

The domain they use is  $\Omega = [0, \pi]$  and they use units such that  $\epsilon_0 = \mu_0 = 1$ . In the 1st case  $\epsilon_r(t) = (1+t)^2$ ,  $J(t, x) = 0$ ,  $E_z(0, x) = \sin x$  and  $H_y(0, x) = -\frac{\cos x}{2}$ . With these initial conditions the exact solution of the system is:

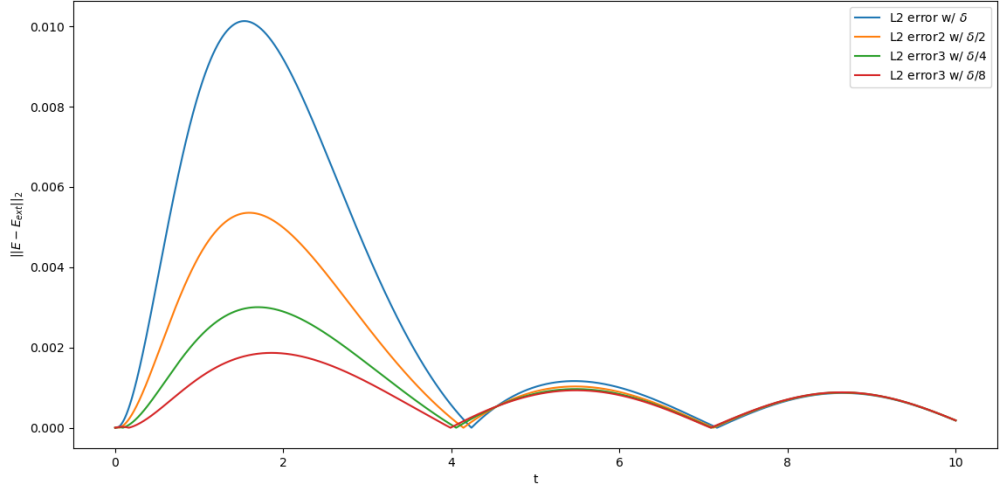
$$\begin{cases} E_z(t, x) = (1+t)^{-3/2} \cos\left(\frac{\sqrt{3}\ln(1+t)}{2}\right) \sin(x) \\ H_z(t, x) = \frac{1}{2\sqrt{1+t}} \left[ -\cos\left(\frac{\sqrt{3}\ln(1+t)}{2}\right) + \sqrt{3} \sin\left(\frac{\sqrt{3}\ln(1+t)}{2}\right) \right] \cos(x) \end{cases}$$

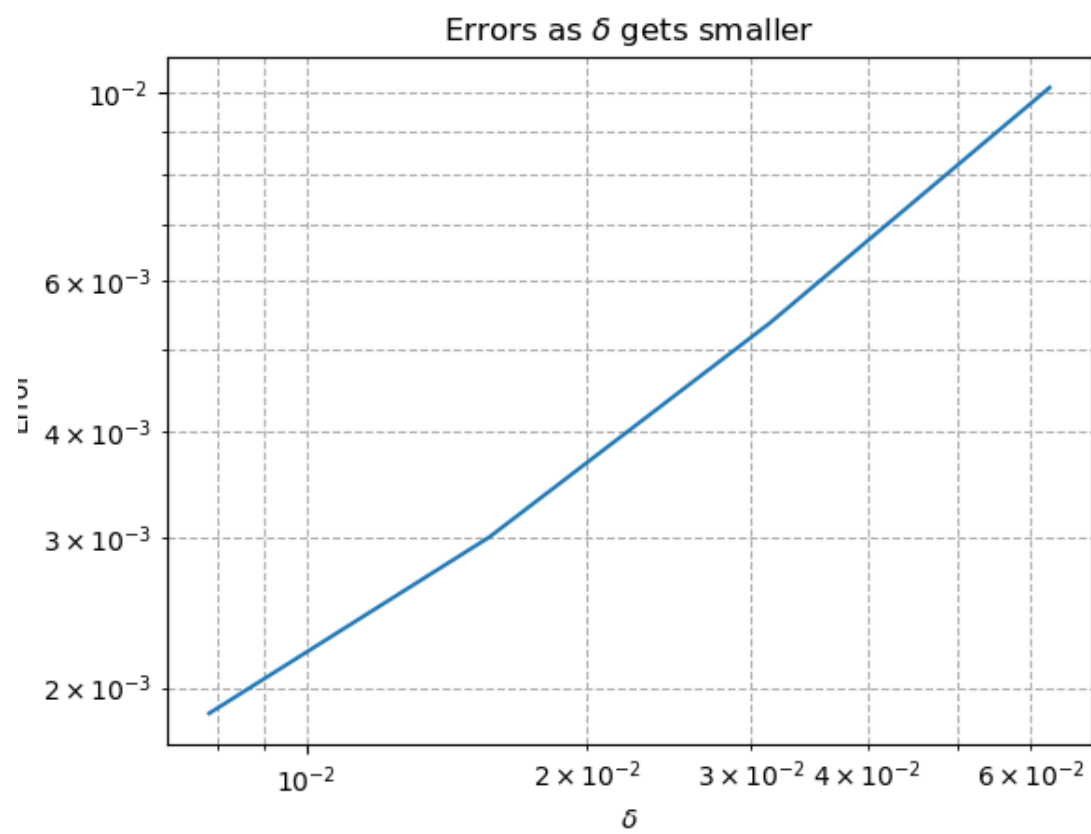
In the 2nd case  $\epsilon_r(t) = e^t$ ,  $J(t, x) = (e^t(\sin t - \cos t) - \sin t) \sin x$ ,  $E_z(0, x) = \sin x$  and  $H_y(0, x) = 0$

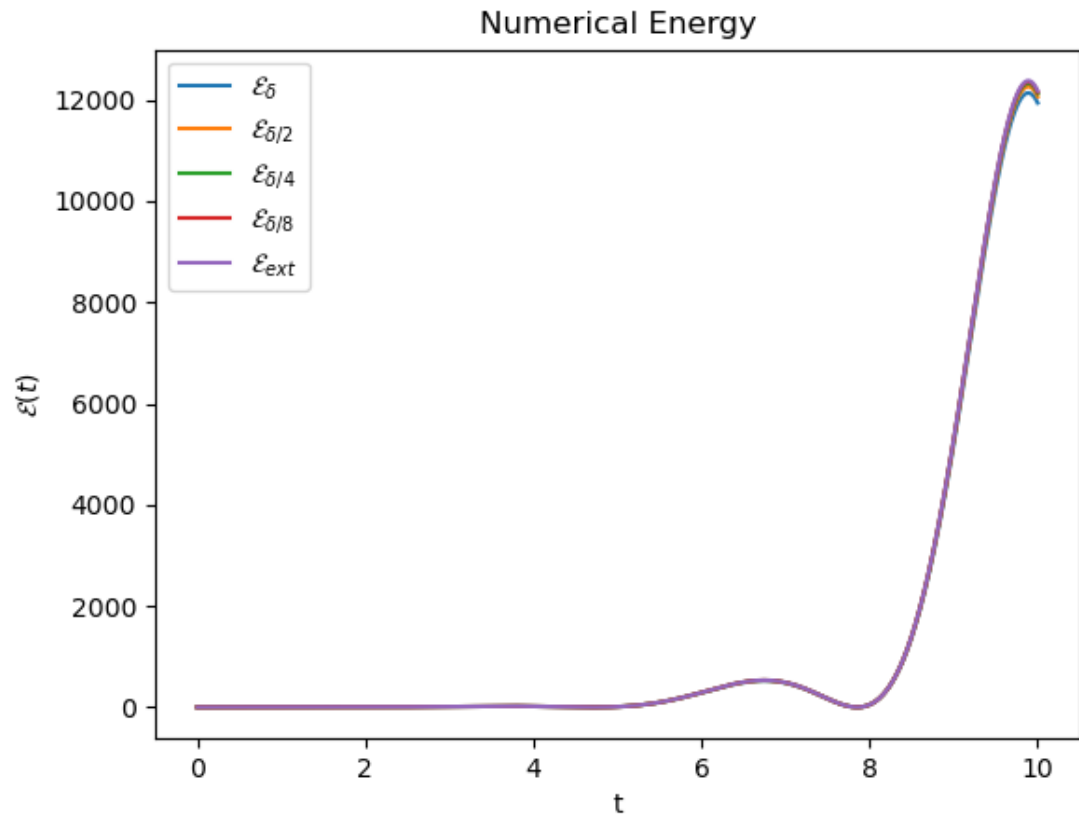
The solutions are:

$$\begin{cases} E_z(t, x) = \cos t \sin x \\ H_z(t, x) = \sin t \cos x \end{cases}$$

I chose to use the 2nd case to analyze the convergence of my implementation. I use as parameters  $\delta = \frac{\pi}{50}$  and  $\Delta t = 0.001$ .







The rate of convergence in this case is only around 0.8. The error plot is not what is expected because we can see that the errors oscillate and decrease while we would expect that they increase.

## 4 Discontinuous Galerkin method in 1D

DG Method can be seen as a finite element method for which we allow discontinuities at borders of elements. Some of the work presented in this section is inspired by [3].

### 4.1 Re-normalized equations

We recall that Maxwell's equations in 1D without current density are:

$$\begin{cases} \partial_x E_z(t, x) = \mu_0 \partial_t H_y(t, x) \\ \partial_x H_y(t, x) = \partial_t(\epsilon(t, x) E_z(t, x)) \end{cases}$$

We re-use the normalized field  $\tilde{E}_z$  and we substitute  $t$  by  $\tilde{t} = ct$  Maxwell's equations become:

$$\begin{cases} \partial_x \tilde{E}_z(\tilde{t}, x) = \partial_{\tilde{t}} H_y(\tilde{t}, x) \\ \partial_x H_y(\tilde{t}, x) = \partial_{\tilde{t}}(\epsilon_r(\tilde{t}, x) \tilde{E}_z(\tilde{t}, x)) \end{cases}$$

For simplicity we will drop all the tilde notation.

We will use conservative variable  $D_z(t, x) = \epsilon_r(t, x) E_z(t, x)$  instead of  $E$ , so we have:

$$\begin{cases} \partial_t D_z = \partial_x H_y \\ \partial_t H_y = \partial_x(\epsilon_r^{-1} D_z) \end{cases}$$

### 4.2 Conservative form

We will now rewrite this system in a conservative form. Let  $\mathbf{u} = \begin{bmatrix} D_z \\ H_y \end{bmatrix}$ . Maxwell's equations can be rewritten in the following way:

$$\partial_t \mathbf{u} + \partial_x(F(\mathbf{u})) = 0$$

$$\text{with } F(\mathbf{u}) = \begin{bmatrix} -H_y \\ -\epsilon_r^{-1} D_z \end{bmatrix} = \begin{bmatrix} 0 & -1 \\ -\epsilon_r^{-1} & 0 \end{bmatrix} \mathbf{u} = \mathbb{A} \mathbf{u}$$

The eigenvalues of  $\mathbb{A}$  are  $\pm \frac{1}{\sqrt{\epsilon_r}} \in \mathbb{R}$  which mean that our system is hyperbolic.

### 4.3 Weak formulation

As in FEM method DG starts by rewriting the problem in a weak formulation. Let  $\Omega = [0, L]$  our domain and  $\{I_k = ]x_k, x_{k+1}[ \}_{k \in \llbracket 0, n-1 \rrbracket}$  intervals in  $\Omega$  such that  $\bigcup_k I_k = \Omega - \{x_k\}_k$  and  $I_k \cap I_j = \emptyset$  if  $k \neq j$ . Let  $V = H^1(\Omega)$ . The weak formulation of our problem is:

Find  $\mathbf{u} \in C^1([0, T], V^2)$  such that:  $\forall k \in \llbracket 0, n-1 \rrbracket, \forall \psi \in V$

$$\begin{aligned} \int_{I_k} \partial_t \mathbf{u} \psi + \partial_x F(\mathbf{u}) \psi dx &= 0 \\ \iff \\ \int_{I_k} \partial_t \mathbf{u} \psi - F(\mathbf{u}) \partial_x \psi dx &= -[F(\mathbf{u}) \psi]_{x_k}^{x_{k+1}} \end{aligned}$$

The right hand side term is called the flux-term and it is the term that connects the intervals to each others.

### 4.4 Space discretization

The idea in Galerkin's method to solve the weak formulation numerically is to approximate the space of function  $V$  with a finite dimensional space  $V_h$ . In our case we will take:  $V_h = \{v \in L^2(\Omega) : v|_{I_k} \in \mathbb{P}^d(I_k)\}$  where  $\mathbb{P}^d(I_k)$  is the space of polynomials of degree less than  $d$  on  $I_k$ . We need also to approximate the right-hand side of the equation because our solution can be discontinuous at the points  $x_k$ . This approximation is called the numerical flux. We choose to take the central numerical flux which is:

$$F^*(\mathbf{u}_k^+, \mathbf{u}_k^-) = \frac{F(\mathbf{u}_k^+) + F(\mathbf{u}_k^-)}{2}$$

where  $\mathbf{u}_k^+ = \lim_{x \rightarrow x_k^+} \mathbf{u}(x)$  and  $\mathbf{u}_k^- = \lim_{x \rightarrow x_k^-} \mathbf{u}(x)$ .

Let  $\{\phi_{ki}\}_{i \in \llbracket 0, d \rrbracket}$  a basis of  $\mathbb{P}^d(I_k)$  and  $\mathbf{u}_k = \mathbf{u}|_{I_k}$ .

If we take  $\mathbf{u} \in C^1([0, T], V_h^2)$  then we can write:

$$\mathbf{u}_k(x, t) = \sum_{i=0}^d \mathbf{c}_{ki}(t) \phi_{ki}(x) = \begin{bmatrix} u_{1k} \\ u_{2k} \end{bmatrix}$$

$$\text{Let } \mathbf{c}_k = \begin{bmatrix} (c_{1ki})_{i \in \llbracket 0, d \rrbracket}^T \\ (c_{2ki})_{i \in \llbracket 0, d \rrbracket}^T \end{bmatrix} = \begin{bmatrix} \mathbf{c}_{1k} \\ \mathbf{c}_{2k} \end{bmatrix}$$

The approximated weak formulation is then:

Find  $\mathbf{c}_k \in \mathcal{C}^1([0, T], \mathbb{R}^{2d+2})$  such that:  $\forall j \in \llbracket 0, d \rrbracket$  :

$$\int_{I_k} \partial_t \mathbf{u}_k \phi_{kj} - F(\mathbf{u}_k) \partial_x \phi_{kj} dx = -[F^*(\mathbf{u}_l^+, \mathbf{u}_l^-) \phi_{kj}(x_l)]_{l=k}^{l=k+1}$$

## 4.5 Matrix formulation

Let's focus on the 1st component of  $\mathbf{u}_k$ .

Let's compute the integral with the time derivative term:

$$\int_{I_k} \partial_t u_{1k} \phi_{kj} dx = \int_{I_k} \sum_{i=0}^d \dot{c}_{1ki} \phi_{ki} \phi_{kj} dx = \sum_{i=0}^d \dot{c}_{1ki} \int_{I_k} \phi_{ki} \phi_{kj} dx = (\mathbb{M}_k \dot{\mathbf{c}}_{1k})_j$$

where  $\mathbb{M}_k = (\int_{I_k} \phi_{ki} \phi_{kj} dx)$

We call  $\mathbb{M}_k$  the mass matrix of the element  $k$ .

Let's compute the integral with the spatial derivative on  $\phi_{kj}$ .

The flux term can be expressed as :  $F(\mathbf{u}_k)_1 = a_{11} u_{1k} + a_{12} u_{2k}$

so we have:

$$\begin{aligned} \int_{I_k} F(\mathbf{u}_k)_1 \partial_x \phi_{kj} dx &= \int_{I_k} a_{11} u_{1k} \partial_x \phi_{kj} dx + \int_{I_k} a_{12} u_{2k} \partial_x \phi_{kj} dx \\ &= \sum_{i=0}^d c_{1ki} \int_{I_k} a_{11} \phi_{ki} \phi_{kj} dx + \sum_{i=0}^d c_{2ki} \int_{I_k} a_{12} \phi_{ki} \phi_{kj} dx \\ &= (\mathbb{K}_k^{11} \mathbf{c}_{1k} + \mathbb{K}_k^{12} \mathbf{c}_{2k})_j \end{aligned}$$

where  $\mathbb{K}_k^{lm} = (\int_{I_k} a_{lm} \phi_{ki} \partial_x \phi_{kj} dx)_{ij}$

We call  $\mathbb{K}_k^{lm}$  the stiffness matrix of the element  $k$ .

Now we focus on the right-hand side term.

We have:  $(F^*(u_k^+, u_k^-))_1 = \frac{a_{11} u_{1k}^+ + a_{12} u_{2k}^+ + a_{11} u_{1k}^- + a_{12} u_{2k}^-}{2}$

Actually we have :  $u_{ik}^- = u_{i,k-1}(x_k)$  and  $u_{ik}^+ = u_{ik}(x_k)$

so :

$$\begin{aligned}
\frac{1}{2}[\phi_{kj}(x_l)a_{1m}(x_l)u_{ml}^+]_k^{k+1} &= \frac{1}{2}\sum_{i=0}^d \phi_{kj}(x_{k+1})a_{1m}(x_{k+1})c_{m,k+1,i}\phi_{k+1,i}(x_{k+1}) \\
&\quad - \frac{1}{2}\sum_{i=0}^d \phi_{kj}(x_k)a_{1m}(x_k)c_{m,k,i}\phi_{k,i}(x_k) \\
\frac{1}{2}[\phi_{kj}(x_l)a_{1m}(x_l)u_{ml}^-]_k^{k+1} &= \frac{1}{2}\sum_{i=0}^d \phi_{kj}(x_{k+1})a_{1m}(x_{k+1})c_{m,k,i}\phi_{k,i}(x_{k+1}) \\
&\quad - \frac{1}{2}\sum_{i=0}^d \phi_{kj}(x_k)a_{1m}(x_k)c_{m,k-1,i}\phi_{k,i}(x_k)
\end{aligned}$$

We can combine all theses terms in a matrix form:

$$[F^*(\mathbf{u}_l^+, \mathbf{u}_l^-)_1 \phi_{kj}(x_l)]_{l=k}^{l=k+1} = \mathbb{S}_{k11}^1 \mathbf{c}_{1k} + \mathbb{S}_{k11}^2 \mathbf{c}_{1,k+1} - \mathbb{S}_{k11}^3 \mathbf{c}_{1,k-1} + \mathbb{S}_{k12}^1 \mathbf{c}_{2k} + \mathbb{S}_{k12}^2 \mathbf{c}_{2,k+1} - \mathbb{S}_{k12}^3 \mathbf{c}_{2,k-1}$$

where

$$\begin{aligned}
\mathbb{S}_k^{1,lm} &= (\frac{1}{2}(a_{lm}(x_{k+1})\phi_{ki}(x_{k+1})\phi_{kj}(x_{k+1}) - a_{lm}(x_k)\phi_{kj}(x_k)\phi_{ki}(x_k)))_{ij} \\
\mathbb{S}_k^{2,lm} &= (\frac{a_{lm}(x_{k+1})}{2}\phi_{kj}(x_{k+1})\phi_{k+1,i}(x_{k+1}))_{ij} \\
\mathbb{S}_k^{3,lm} &= (\frac{a_{lm}(x_k)}{2}\phi_{kj}(x_k)\phi_{k-1,i}(x_k))_{ij}
\end{aligned}$$

They are the flux matrices.

Now we define general mass, stiffness and flux matrices to express our semi-discrete scheme in a compact manner.

$$\begin{aligned}
\bar{\mathbb{M}}_k &= \begin{bmatrix} \mathbb{M}_k & \mathbb{O} \\ \mathbb{O} & \mathbb{M}_k \end{bmatrix} \\
\bar{\mathbb{K}}_k &= \begin{bmatrix} \mathbb{K}_k^{11} & \mathbb{K}_k^{12} \\ \mathbb{K}_k^{21} & \mathbb{K}_k^{22} \end{bmatrix} \\
\bar{\mathbb{S}}_k^i &= \begin{bmatrix} \mathbb{S}_k^{i,11} & \mathbb{S}_k^{i,12} \\ \mathbb{S}_k^{i,21} & \mathbb{S}_k^{i,22} \end{bmatrix}
\end{aligned}$$

where  $\mathbb{O}$  is the  $d \times d$  null matrix.

Our system is then finally:

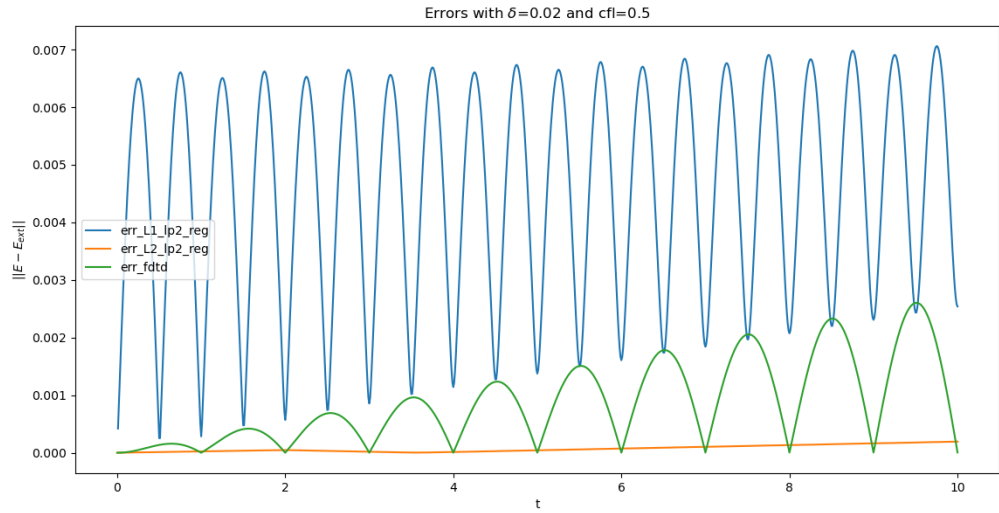
$$\bar{\mathbb{M}}_k \dot{\mathbf{c}}_k - \bar{\mathbb{K}}_k \mathbf{c}_k = -\bar{\mathbb{S}}_k^1 \mathbf{c}_k - \bar{\mathbb{S}}_k^2 \mathbf{c}_{k+1} + \bar{\mathbb{S}}_k^3 \mathbf{c}_{k-1}$$

## 4.6 Comparison with FDTD

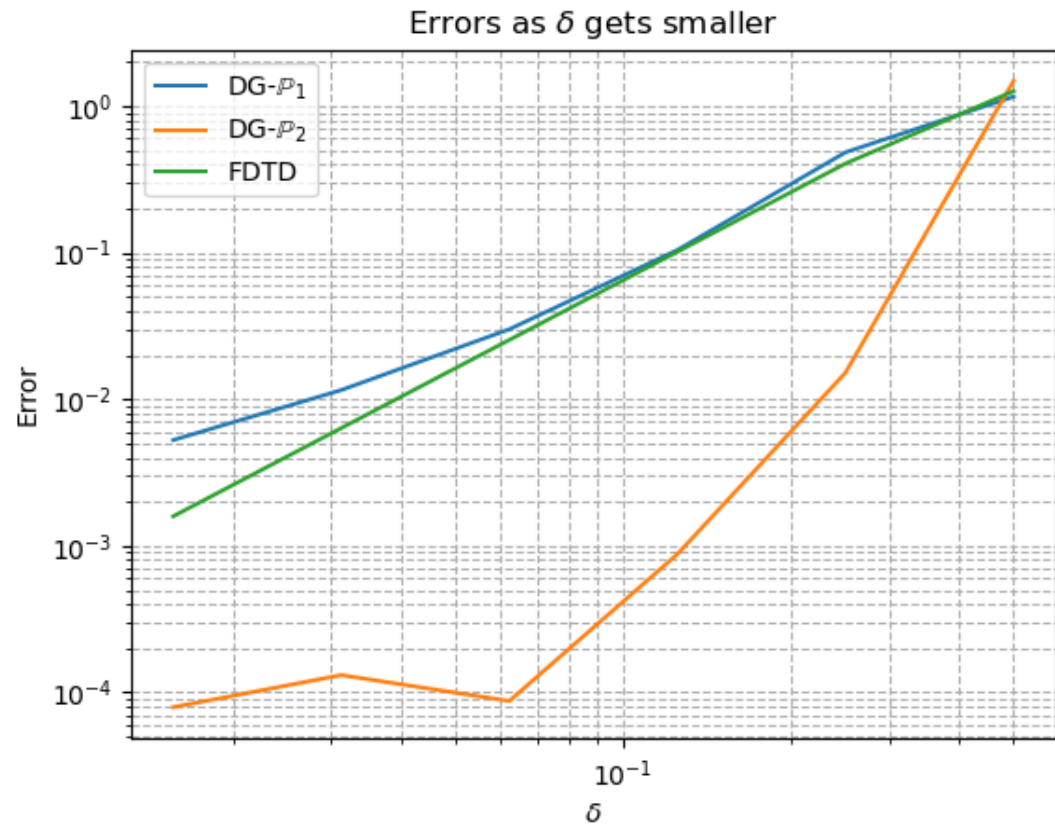
For this part I used a Fortran implementation of the Galerkin scheme and made  $\epsilon$  vary in time in the code. The implementation uses Lagrange polynomials as basis and we can choose the order of the polynomials. For the time integration we use the Leap-Frog algorithm of order 2 because it is what is used in FDTD.

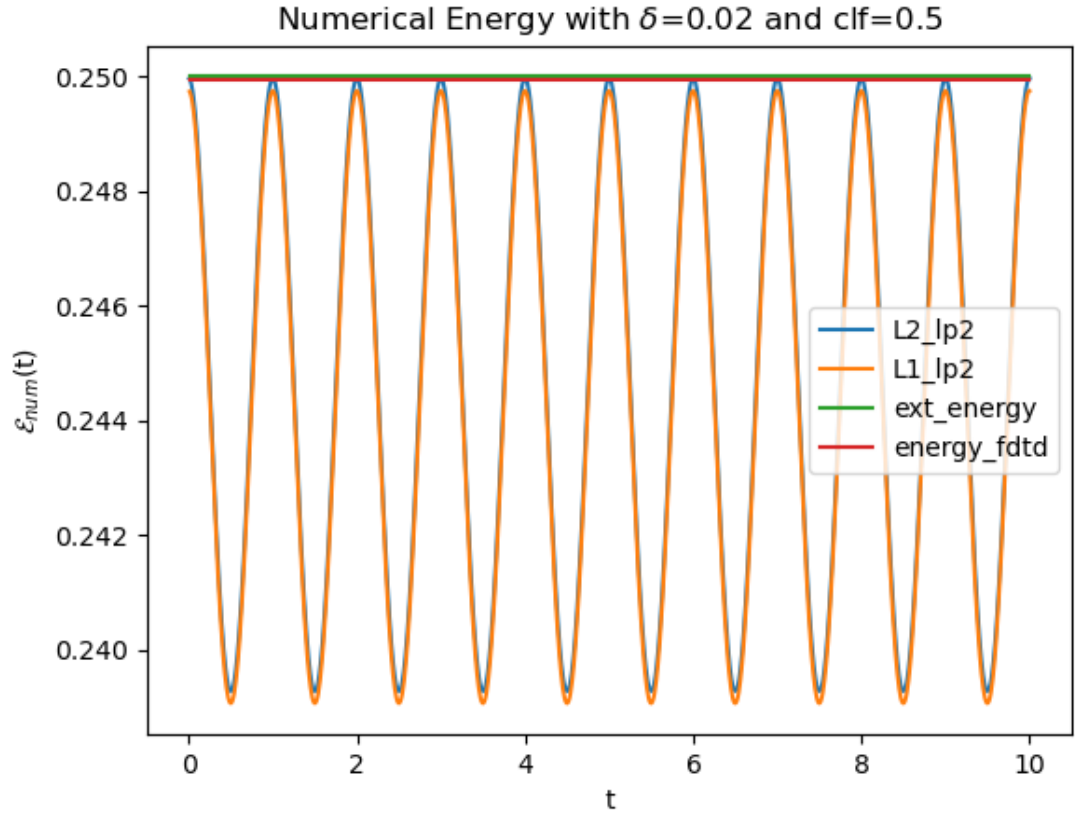
We re-use the case in subsubsection 3.7.1 with  $\delta=1/50$  and a cfl number equal to  $1/2$ .

The results are:







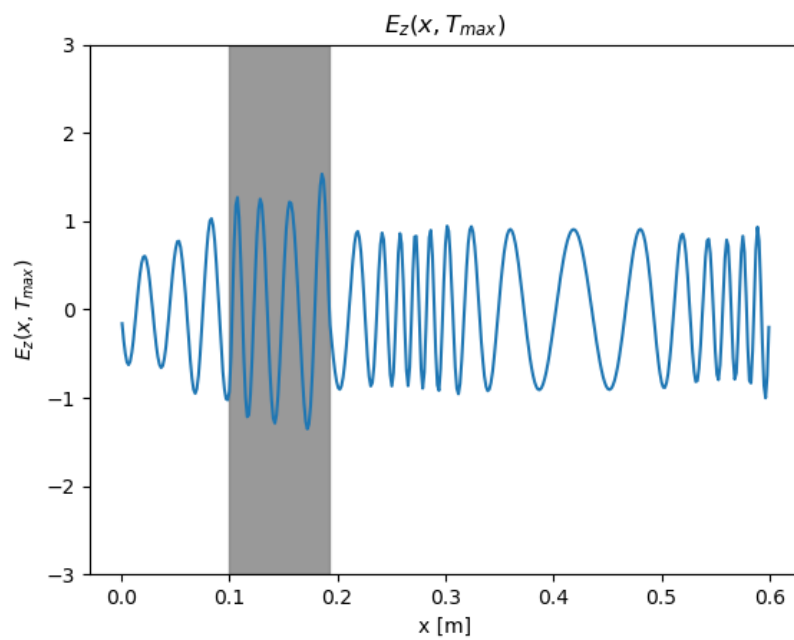
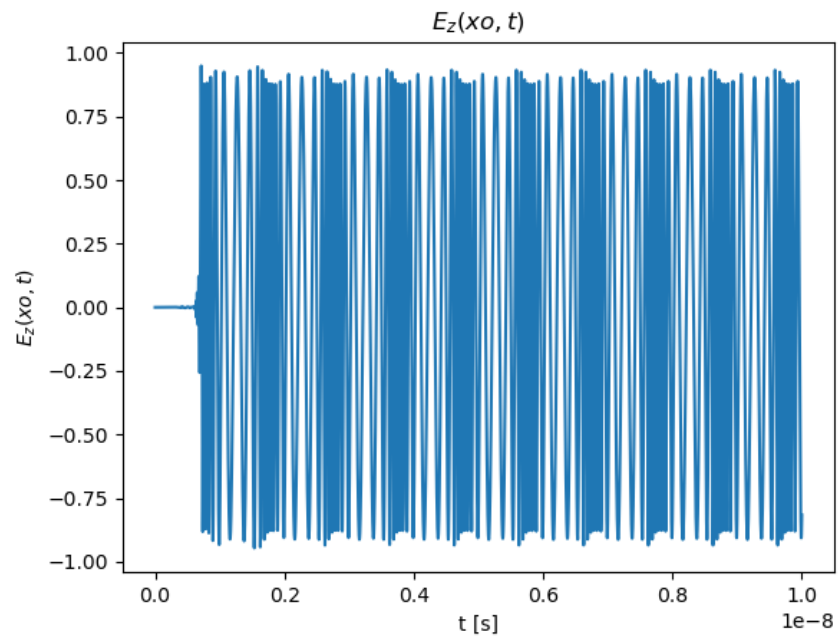


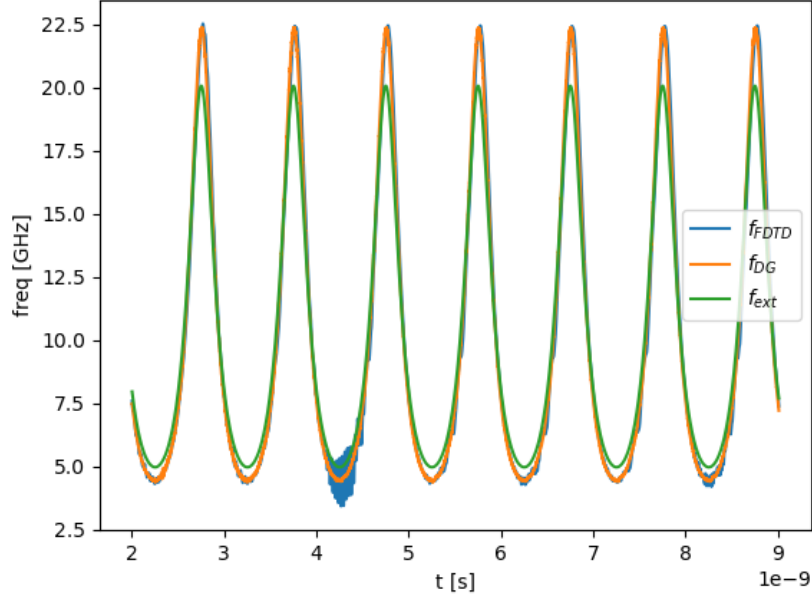
We can see that FDTD has slightly better results than  $DG-P^1$  and has a similar rate of convergence (the rate of convergence of  $DG-P^1$  is 1.7). In the other hand  $DG-P^1$  has way better results and his rate of convergence is 2.4. The energies of  $DG-P^1$  and  $DG-P^2$  are very similar and are not constant contrarily to FDTD.

#### 4.7 Test on a dielectric case

For this part we test the  $DG-P^1$  algorithm on the 1D case presented in [2]. We chose  $\delta = 1.5mm$  and  $clf = 0.1$ .

For the thick slab (93 mm) and a modulation depth equal to 0.67 we obtain:





We can see that we don't have the amplitude modulation we observed using FDTD. We can then conclude that there's might an error in my implementation of FDTD. The frequencies part is however identical.

## 5 Conclusion

During this internship we successfully implemented the FDTD algorithm presented in [2] to simulate Maxwell's equations in time varying media. Except of an amplitude modulation observed with the thick slab our result were identical to the ones presented in [2]. I measured the effectiveness of this implementation using analytical solutions in simple cases. I also added time dependency in a Discontinuous Galerkin implementation, made the same tests as with FDTD and compared both algorithms. The code I made is available at this [link](#).

## References

- [1] István Faragó, Ágnes Havasi, and Robert Horváth. “Numerical solution of the Maxwell equations in time-varying media using Magnus expansion”. In: *Central European Journal of Mathematics* 10.1 (2012), pp. 137–149.
- [2] Xiaowen Liu. “The use of the FDTD method for electromagnetic analysis in the presence of time-varying media”. PhD thesis. University of Ottawa (Canada), 2004.
- [3] Jonathan Viquerat. “Simulation of electromagnetic waves propagation in nano-optics with a high-order discontinuous Galerkin time-domain method”. PhD thesis. Université Nice Sophia Antipolis, 2015.